AFRL-IF-RS-TR-2005-387
Final Technical Report
December 2005

LABORATORY TESTING, CHARACTERIZATION AND MATHEMATICAL MODELING OF THE MONIWRIST III BY ROSS-HIME DESIGNS, INCORPORATED

Advanced Technical Concepts

APPROVED FOR PUBLIC RELEASE; DISTRIBUTION UNLIMITED.

AIR FORCE RESEARCH LABORATORY
INFORMATION DIRECTORATE
ROME RESEARCH SITE
ROME, NEW YORK

STINFO FINAL REPORT

This report has been reviewed by the Air Force Research Laboratory, Information Directorate, Public Affairs Office (IFOIPA) and is releasable to the National Technical Information Service (NTIS). At NTIS it will be releasable to the general public, including foreign nations.

AFRL-IF-RS-TR-2005-387 has been reviewed and is approved for publication

APPROVED: /s/

DON J. NICHOLSON
Project Engineer

FOR THE DIRECTOR: /s/

WARREN H. DEBANY, JR., Technical Advisor
Information Grid Division
Information Directorate

REPORT DOCUMENTATION PAGE

Form Approved
OMB No. 074-0188

1. AGENCY USE ONLY (Leave blank)	2. REPORT DATE	3. REPORT TYPE AND DATES COVERED
	DECEMBER 2005	Final Sep 02 – Dec 02

4. TITLE AND SUBTITLE
LABORATORY TESTING, CHARACTERIZATION AND MATHEMATICAL MODELING OF THE MONIWRIST III BY ROSS-HIME DESIGNS, INCORPORATED

5. FUNDING NUMBERS
C - F30602-02-1-0220
PE - 62702F
PR - 558B
TA - II
WU - RS

6. AUTHOR(S)
Victor A. Skormin

7. PERFORMING ORGANIZATION NAME(S) AND ADDRESS(ES)
Advanced Technical Concepts
352 Hill Road
Berkshire New York 13736

8. PERFORMING ORGANIZATION REPORT NUMBER
N/A

9. SPONSORING / MONITORING AGENCY NAME(S) AND ADDRESS(ES)
Air Force Research Laboratory/IFGC
525 Brooks Road
Rome New York 13441-4505

10. SPONSORING / MONITORING AGENCY REPORT NUMBER
AFRL-IF-RS-TR-2005-387

11. SUPPLEMENTARY NOTES

AFRL Project Engineer: Don J. Nicholson/IFGC/(315) 330-7437/Donald.Nicholson@rl.af.mil

12a. DISTRIBUTION / AVAILABILITY STATEMENT
APPROVED FOR PUBLIC RELEASE; DISTRIBUTION UNLIMITED.

12b. DISTRIBUTION CODE

13. ABSTRACT ***(Maximum 200 Words)***

The Omni-Wrist III gimbal system, developed by Ross-Hime Designs, Inc. has been fully tested in the Laser Research Laboratory of Binghamton University. This emulates the kinematics of the human wrist, allowing a full 180 degree hemisphere of pitch/yaw motion. A complete mathematical model (transfer matrix) was developed, which demonstrated the potential for greatly improved bandwidth and positioning accuracy. It is proposed to enhance the system performance through development of an optimal comptroller extending the conventional state-variable and model reference control laws, with dynamic programming, gain scheduling and fuzzy logic.

14. SUBJECT TERMS
Satellite, Communication, Pointing

15. NUMBER OF PAGES
30

16. PRICE CODE

17. SECURITY CLASSIFICATION OF REPORT	18. SECURITY CLASSIFICATION OF THIS PAGE	19. SECURITY CLASSIFICATION OF ABSTRACT	20. LIMITATION OF ABSTRACT
UNCLASSIFIED	UNCLASSIFIED	UNCLASSIFIED	UL

Table of Contents

List of Figures

1. Introduction

Omniwrist III is a new sensor mount developed under Air Force funding that emulates the kinematics of a human wrist. Driven by two linear motors and computer controlled, it is capable of a full 180° hemisphere of pitch/yaw motion. A comprehensive laboratory testing of one of few existing devices of this type, installed in the Laser Research Laboratory at Binghamton University, has resulted in the establishment of a complete transfer matrix-type model relating pitch/yaw coordinates of the sensor mount to the voltage signals applied to the motors. While the dynamic characteristics of the device are position-dependent, the transfer matrix was supplied with an array of parameters, representing various points of its operation on the sphere. It was found that the device has the potential for exceeding bandwidth and positioning accuracy of a traditional Schaeffer gimbals system at least by the factor of ten. The device is suitable for the application of the most advanced control strategies that will result in the further enhancement of its dynamic performance thus extending the scope of its application to various problems of satellite communications, LADAR, laser weapon systems, etc.

This study is aimed at the investigation of the best performance characteristics (bandwidth, tracking error, cross-coupling effects, power consumption, etc.) attainable under the conventional, state-variable and model reference control laws. It is shown that Omniwrist III with the appropriate controls could be considered as a new generation of gimbals system.

It is proposed **to continue this study** investigating the application aspects and performance enhancement of the Omniwrist system due to optimal controller utilizing dynamic programming, gain scheduling, and fuzzy logic controller that will be first synthesized using the developed mathematical model, and later implemented in the dedicated computer of the Omniwrist. Implemented in software and in hardware, these control strategies should be tested in such typical laser positioning applications as agile repositioning of the laser beam, tracking a moving target, scanning, and offsetting vibration of the optical platform. Design and comprehensive investigation of a hybrid laser beam positioning system comprising the Omniwrist for the coarse steering task and an acousto-optic Bragg cell for fine steering is **also proposed**.

2. Mathematical Description of the Omniwrist Gimbals System

An innovative robotic wrist design by Ross-Hime Designs, Inc provides an alternative to traditional 2-axis gimbals positioners 0. A full hemisphere range is covered by two linear motors and a series of joints constituting the Omni-Writst III free-space laser communications sensor mount (Figure 1), providing singularity-free pointing capability for up to 5 lbs of payload. A description of the components will be followed by the development of a mathematical model, building the ground for the analysis and design of control scenarios in the next chapter.

2.1 The Laboratory Setup

The components and their functional interconnections of the Omniwrist setup are shown in Figure 2. A brief exploration of the particular modules with links to sources of more detailed information made available by the manufacturers will be presented in following subsections.

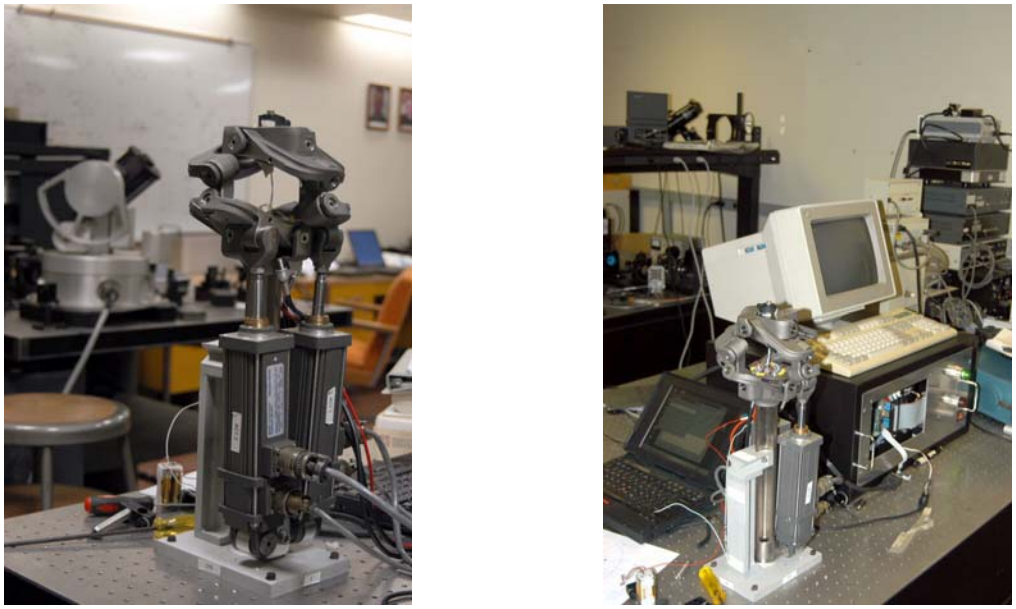

Figure 1 - The Omniwrist III Setup

2.1.1 Dedicated PC

A proprietary Microsoft Windows95 application running on a Pentium-based IBM laptop serves as a user interface of the setup with the ability to calibrate the drive and perform simple positioning tasks. After completing the homing sequence, the device is ready to

accept user input and change the pointing direction based on the given values for azimuth and declination. The control hierarchy and functionality is similar to the Schaeffer gimbals system in that the user interface PC supplies a stand-alone controller with high-level commands containing (step) reference information over a serial connection. The controller in this case is implemented on Ziatech's STD32 Bus based ZT8907 single board computer featuring an Intel DX4 processor 0. A simple interface program running on a Microsoft DOS 6.22 platform receives the serial data from the user interface PC and returns confirmation codes, processes the signals from the calibration switches, converts between the azimuth and declination and encoder signals, and communicates with the servo motion control board, which implements the low-level control.

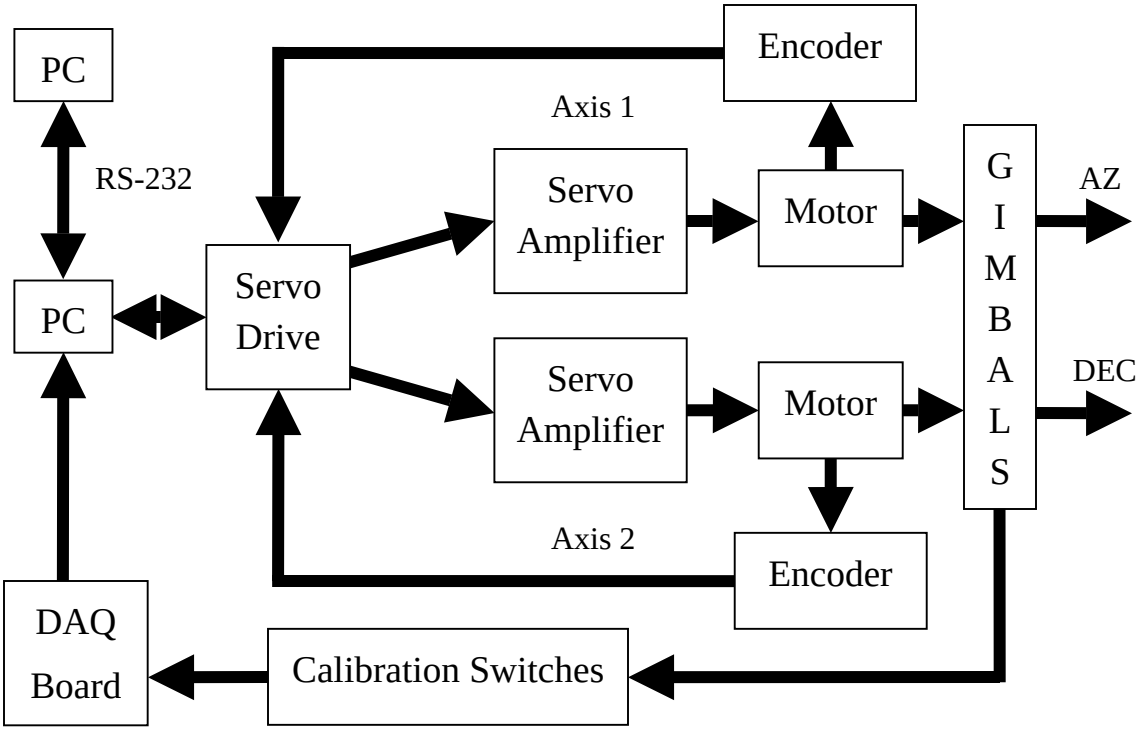

Figure 2 - Components of the Omni-Wrist III Laboratory Setup

2.1.2 Servo Drive

An ACS-Tech80 4-Axes Servo Motion Controller board, model 4350A, connected to the STD32 bus, generates the control signals based on the step reference given by the

interface software 0. The controller board is interfaced with the servo amplifiers as well as the encoders, acquiring the position feedback information.

2.1.3 Servo Amplifier

Advanced Motion Controls SE30A40AC brushless servo amplifiers provide the necessary power and modulation to drive the motors [4].

2.1.4 Motor

The actuation of the gimbals is realized through Exlar Corporation GS-20 series linear brushless motors 0. Embedded within the enclosure of the motors are quadrature optical encoders, supplying incremental position information to the counters on the Motion Controller Board (Servo Drive).

2.1.5 Gimbals

The mechanical design couples the motors with the sensor mount through a series of joints, transforming the motor encoder position vector into azimuth and declination coordinates of the mount.

2.1.6 Calibration Sensors

A Philtec, Inc RC63 fiber optic displacement sensor is a key feedback source in the homing sequence in sensing the calibration position 0. The associated sensor electronics conditions the signals to be intelligible by the DAQ board.

2.1.7 DAQ Board

The analog signal from the calibration sensors is acquired by a VersaLogic Corp VL-1260 12-bit analog input card capable of over 10 kHz sampling frequency [7].

2.2 Experimental Investigation of the Gimbals System

Although the diagram of Figure 2 indicates that the particular modules of the Omniwrist system and their functional interrelationship are similar to the ones of a Schaeffer gimbals systems, there are several fundamental differences between the two systems.

2.2.1 Motor Operation

While the Schaeffer gimbals are actuated by current-driven rotary DC brush motors (with the current proportional to the control input), the Omniwrist is positioned by linear brushless motors, requiring three-phase sinusoidal control signal modulation. Luckily for the designer, the modulation procedure is transparent from the point of view of the control signal due to the use of the brushless servo amplifiers.

2.2.2 Mechanical Design

The modeling and control tasks of the Schaeffer setup are reduced due to the independence of the azimuth and declination channels, which can each be modeled and controlled separately. The Omniwrist kinematical design combines the effect of both motors to form the azimuth and declination coordinates, which will need to be reflected in the model as well as in the control design, where decoupling of the inputs and outputs will be a necessity.

2.2.3 Nonlinearities

The friction in the Omniwrist gimbals appears to be far less significant with respect to the maximum force generated by the motors then in the Schaeffer gimbals, allowing for a greater range of the control input. While an explicit measurement of saturation was not possible (as it is not possible in the Schaeffer gimbals setup), the effects of saturation appear to be far less significant in the Omniwrist system.

2.2.4 Control Input Voltage

The range of control input voltages acceptable by the servo amplifier is limited by – 10 V and + 10 V, which is the same as the range of the inputs of the servo amplifier used in the Schaeffer setup.

2.2.5 Encoder Resolution

The resolution of the encoders was measured to be 20.52 μrad per pulse, more than 4.5 times the resolution of the Schaeffer system encoders, promising drastic accuracy improvement.

2.2.6 Servo Motion Controller

Low-level control is implemented directly on the motion controller board utilizing a trapezoidal velocity envelope generator and a PID velocity controller and featuring a microprocessor, which constantly monitors the performance of the controller and updates the velocity envelope.

2.3 Mathematical Model of the Gimbals System

Due to hardware upgrades coinciding with the analysis and control implementation processes, the modeling task was limited to the static model of the kinematics of the Omniwrist and the coupling between the input and output signals.

2.3.1 Coupling between the Angular and Encoder Signals

The mechanical design of the Omniwrist causes cross coupling between the input and output signals. Voltage applied to only axis #1 of the gimbals results in movement in both the azimuth and the declination directions. Similarly, if only axis #2 is driven by a control signal, the gimbals will move in both the azimuth and the declination directions. Analysis of Figure 3 suggests a complicated interrelationship between the input motor positions (applied at two of the bottom parts) and the outputs (azimuth and declination). Without the knowledge of the parameters of the parts being used, it would be very difficult to come up with the exact model. Therefore, the coupling relationships were inspected in an attempt to find (guess) the underlying mathematical description.

Utilizing a development version of the interface software found on the controller PC, some input/output data was collected by entering a desired azimuth and declination position and reading the equivalent encoder positions on both axes. An inspection of Figure 4, showing the dependence of the encoder position of axis #1 (a) and axis #2 (b) on variations of the azimuth position, indicates that the relationship between the azimuth position and the position of the encoders of both motors can be approximated by trigonometric functions. Furthermore, Figure 5 shows, that the dependence of the encoder position of axis #1 on the declination can be approximated by a sine-function.

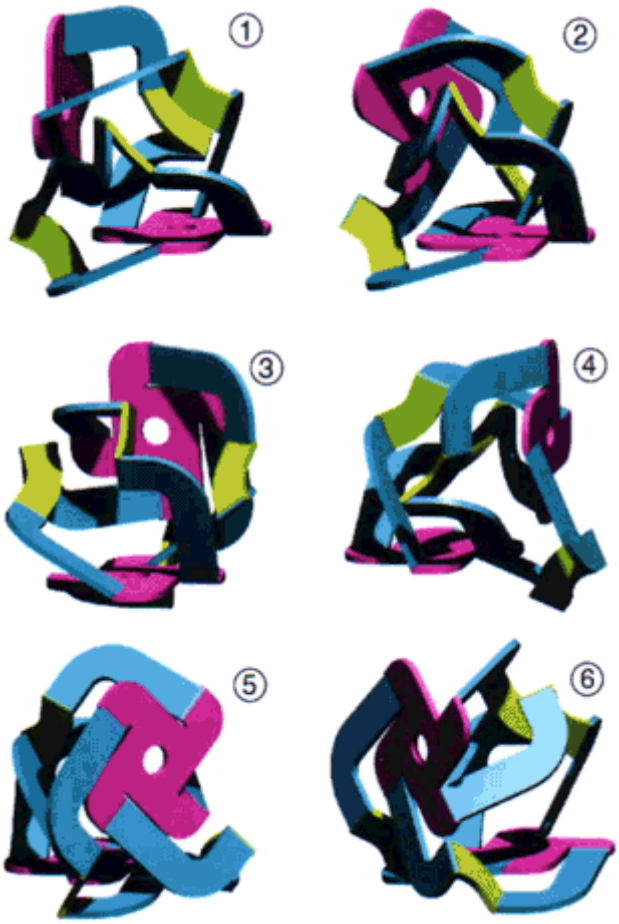

Figure 3 - Kinematics of the Omniwrist III (source: 0)

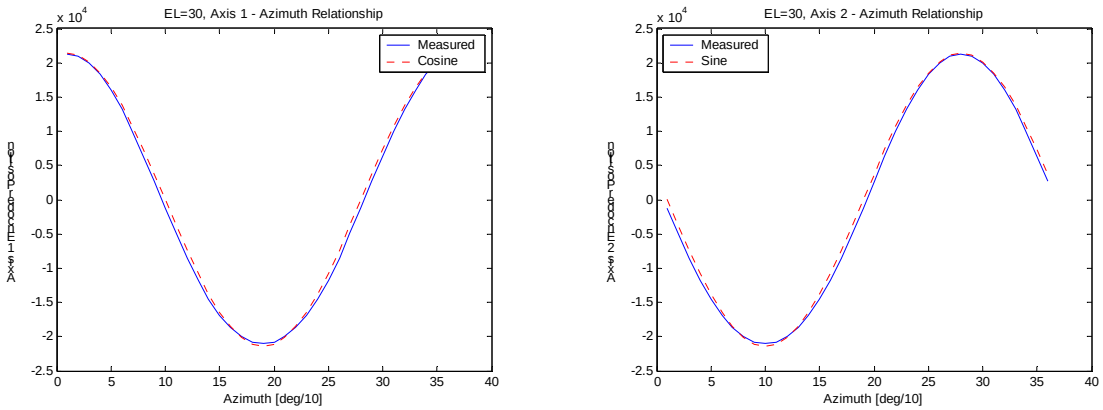

(a) (b)

Figure 4 - Relationship Between Azimuth and Encoder Position of (a) Axis 1 and (b) Axis 2; Declination = 30°

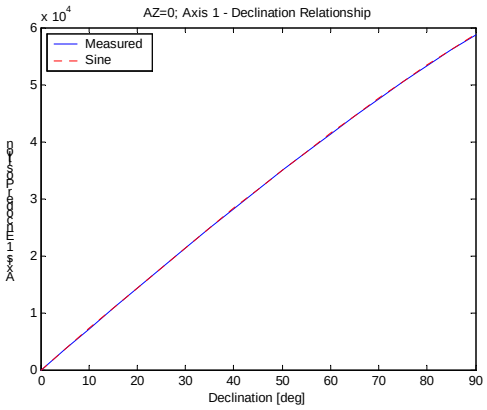

Figure 5 - Relationship Between Declination and Encoder Position of Axis 1

The above findings can be summarized in following equations, whose coefficients were estimated on the basis of input/output data by using a genetic optimization-based [8] Least Squares procedure

$$Ax_1 = 8.524 \cdot 10^3 \cdot \sin(0.4845 \cdot DEC) \cdot \cos(AZ) \text{ and} \tag{1}$$

$$Ax_2 = -8.524 \cdot 10^3 \cdot \sin(0.4845 \cdot DEC) \cdot \sin(AZ). \tag{2}$$

Dividing equation (2) by equation (1) yields

$$\frac{Ax_2}{Ax_1} = -\frac{\sin(AZ)}{\cos(AZ)} = -\tan(AZ), \tag{3}$$

which results in

$$AZ = -\tan^{-1}\left(\frac{Ax_2}{Ax_1}\right) \text{ and} \tag{4}$$

$$DEC = \frac{\sin^{-1}\left(\dfrac{Ax_1}{8.524 \cdot 10^4 \cdot \cos(AZ)}\right)}{0.4845}. \tag{5}$$

2.3.2 Actuator Transfer Functions

In order to build a control system, one needs to have the knowledge of the dynamics of the system to be controlled. Without access to the design documentation, a control engineer needs to conduct experiments, which will provide an estimate of the dynamic

model of the system. This was the case with the Schaeffer gimbals system as well as the Omniwrist III gimbals system.

A series of experiments was conducted, gathering responses of encoders of both axes to positive and negative inputs at 13 different operating points, given by 13 different azimuth and declination pairs. The outcomes of the experiments are shown in Figure 6, indicating different responses at different operating points. An average velocity response of axis #1 and axis #2 along with the 1st order model obtained through the Least Squares estimation is shown in Figure 7. The transfer functions were found to be

$$G_1(s) = \frac{2.3 \cdot 10^6}{s + 36} \text{ and} \tag{6}$$

$$G_2(s) = \frac{1.75 \cdot 10^6}{s + 34}. \tag{7}$$

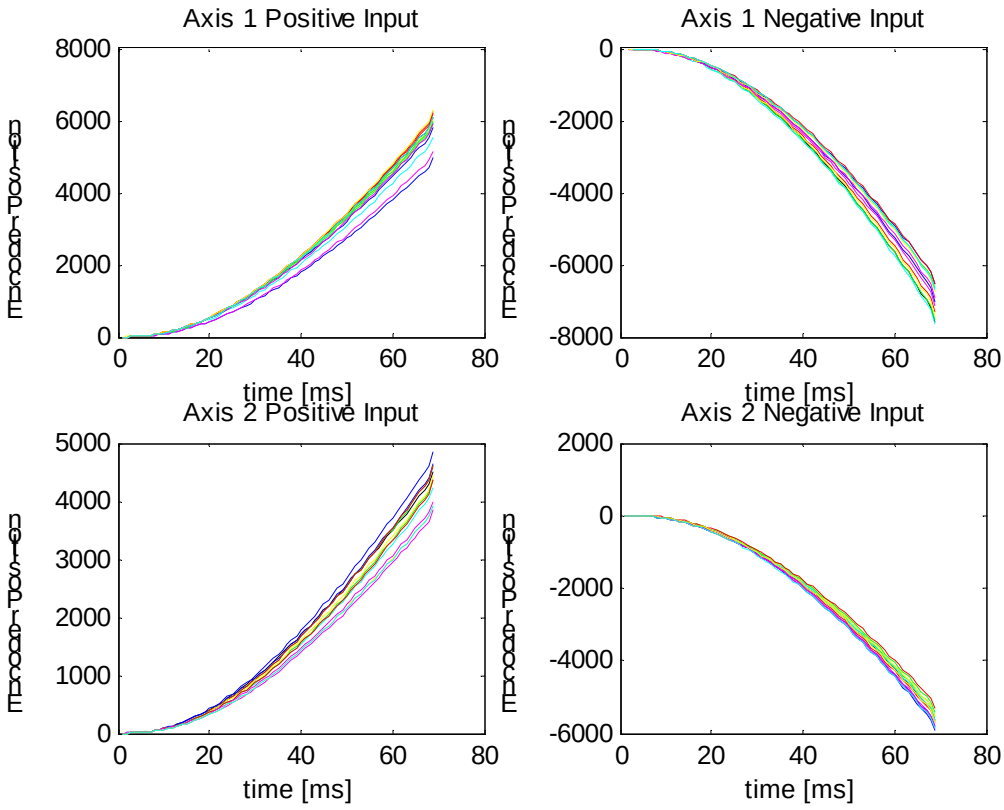

Figure 6 - Responses of Both Motors to Positive and Negative Inputs at Different Operating Points

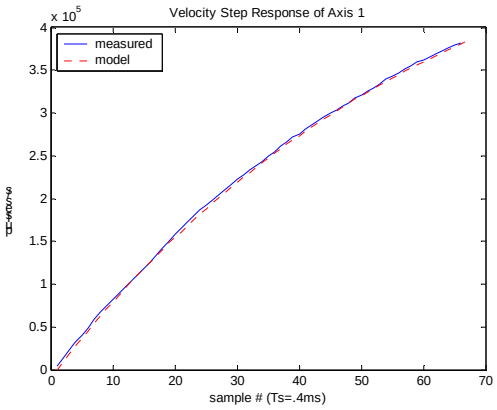

(a)

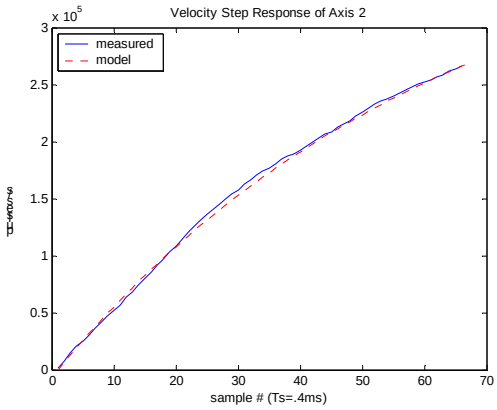

(b)

Figure 7 - Velocity Response of a 1st Order Model of (a) Actuator 1 and (b) Actuator 2

3. Digital Control of the Gimbals System

As it was mentioned earlier, malfunctioning of the Omniwrist hardware has the design and verification of digital controllers to computer simulations. The effort includes the analysis of the existing controller followed by the development of a state-variable and an adaptive model following controller.

3.1 Analysis of the Existing Control System

The functionality of the existing controller as well as its structure are very similar to that of the Schaeffer gimbals. The user enters the desired azimuth and declination position into the software on the interface laptop, which is communicated over a serial link to the single board computer, where the target position is converted into the encoder coordinates and velocity envelopes are generated for both channels. A PID controller and an overseeing microprocessor on the servo motion controller board assure that the system follows the required velocity envelopes. Again, it is only possible to change the desired position after the previous move has completed. Also, similarly to the Schaeffer system, the inaccessibility of the control and feedback signals limits the thoroughness of the system analysis. Apart from the above-mentioned controller structure and its inconvenience for tracking, the original control system exhibits coupling of the outputs, an issue, which will be the main concern of following sections.

3.2 Design, Application and Testing of a State-Variable Controller

Two independent controllers, designed for individual channels as per [9], are shown in Figure 8. Note that the encoder coordinates are not coupled, and the coupling takes place in the blocks filtering the reference and output.

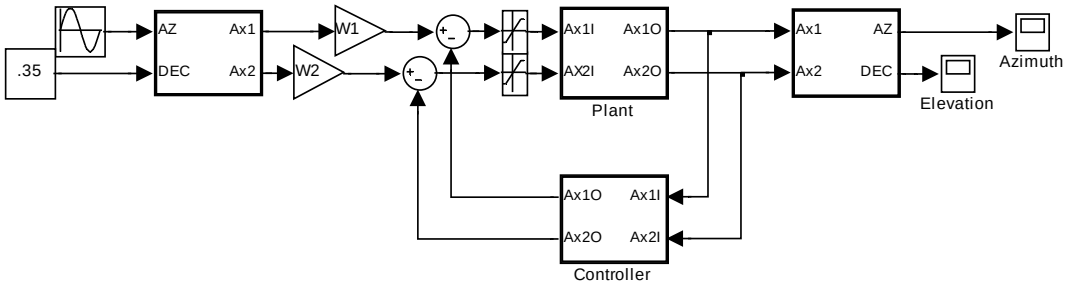

(a)

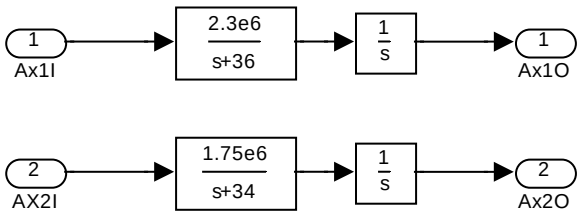

(b)

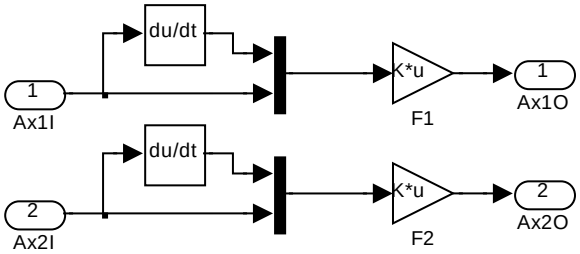

(c)

Figure 8 - Omniwrist State Variable Controller; (a) Overall System; (b) Plant; (c) Controller

The plant, described by transfer functions (6) and (7) can be expressed in state variable form as

$$A = \begin{bmatrix} -36 & 0 & 0 & 0 \\ 1 & 0 & 0 & 0 \\ 0 & 0 & -34 & 0 \\ 0 & 0 & 1 & 0 \end{bmatrix}$$
$$B = \begin{bmatrix} 2.3 \cdot 10^6 & 0 \\ 0 & 0 \\ 0 & 1.75 \cdot 10^6 \\ 0 & 0 \end{bmatrix} \quad (8)$$
$$C = \begin{bmatrix} 0 & 1 & 0 & 0 \\ 0 & 0 & 0 & 1 \end{bmatrix}$$

The desired closed loop system's state variable representation is

$$A = \begin{bmatrix} -80 & -1601 & 0 & 0 \\ 1 & 0 & 0 & 0 \\ 0 & 0 & -80 & -1601 \\ 0 & 0 & 1 & 0 \end{bmatrix}$$
$$B = \begin{bmatrix} 2.3 \cdot 10^6 & 0 \\ 0 & 0 \\ 0 & 1.75 \cdot 10^6 \\ 0 & 0 \end{bmatrix} \quad (9)$$
$$C = \begin{bmatrix} 0 & 1 & 0 & 0 \\ 0 & 0 & 0 & 1 \end{bmatrix}$$

with eigenvalues -40+j and -40-j for each channel. The controller and filter matrices *F* and *W*, which will achieve the desired closed loop performance, were found to be

$$F = \begin{bmatrix} 1.913 & 69.609 & 0 & 0 \\ 0 & 0 & 2.629 & 91.486 \end{bmatrix} \cdot 10^{-5}$$
$$W = \begin{bmatrix} 69.609 & 0 \\ 0 & 91.486 \end{bmatrix} \cdot 10^{-5} \quad (10)$$

The closed-loop step response of the system can be seen in Figure 9.

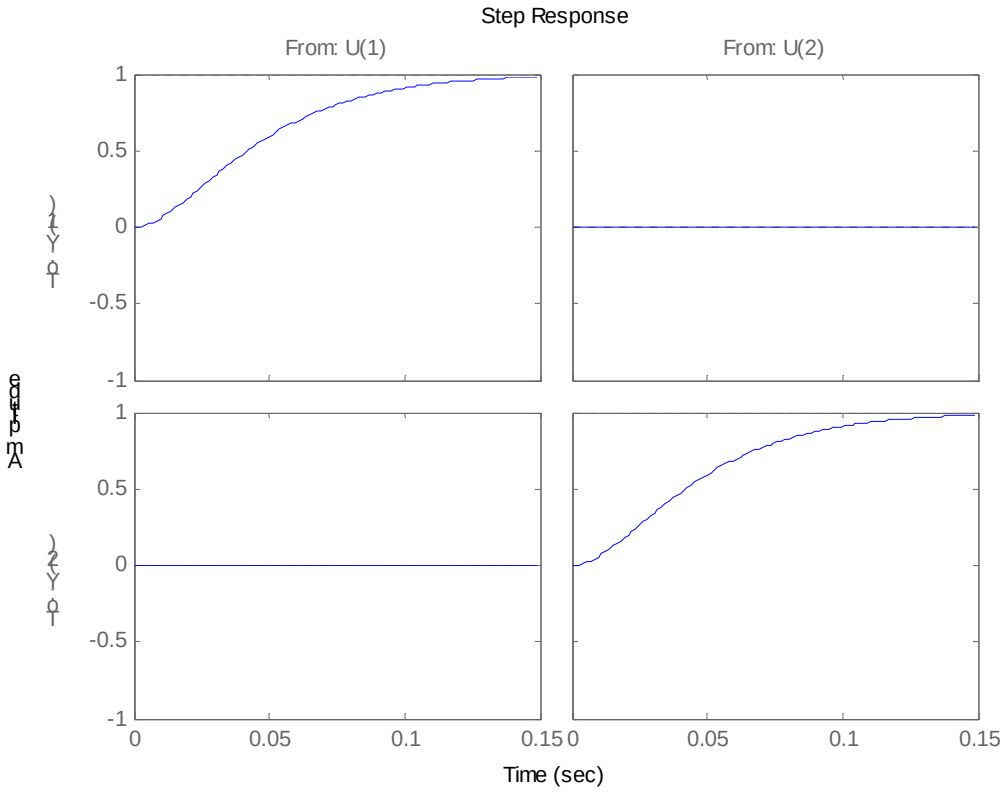

Figure 9 - Closed-Loop System Step Response

To investigate the coupling, the azimuth input was driven with a sinusoidal signal, while the declination was kept constant. Figure 10 (d) reveals the propagation of the azimuth reference into the declination channel. The coupling effect is fairly small, thanks to the slow variation of the reference signal (the system is steady-state decoupled), but could be significant for aerospace applications. Therefore, an adaptive control system was built and investigated for its decoupling capabilities.

Note: The initial error in Figure 10 (e) is due to different initial conditions of the plant and the decoupled closed-loop system model.

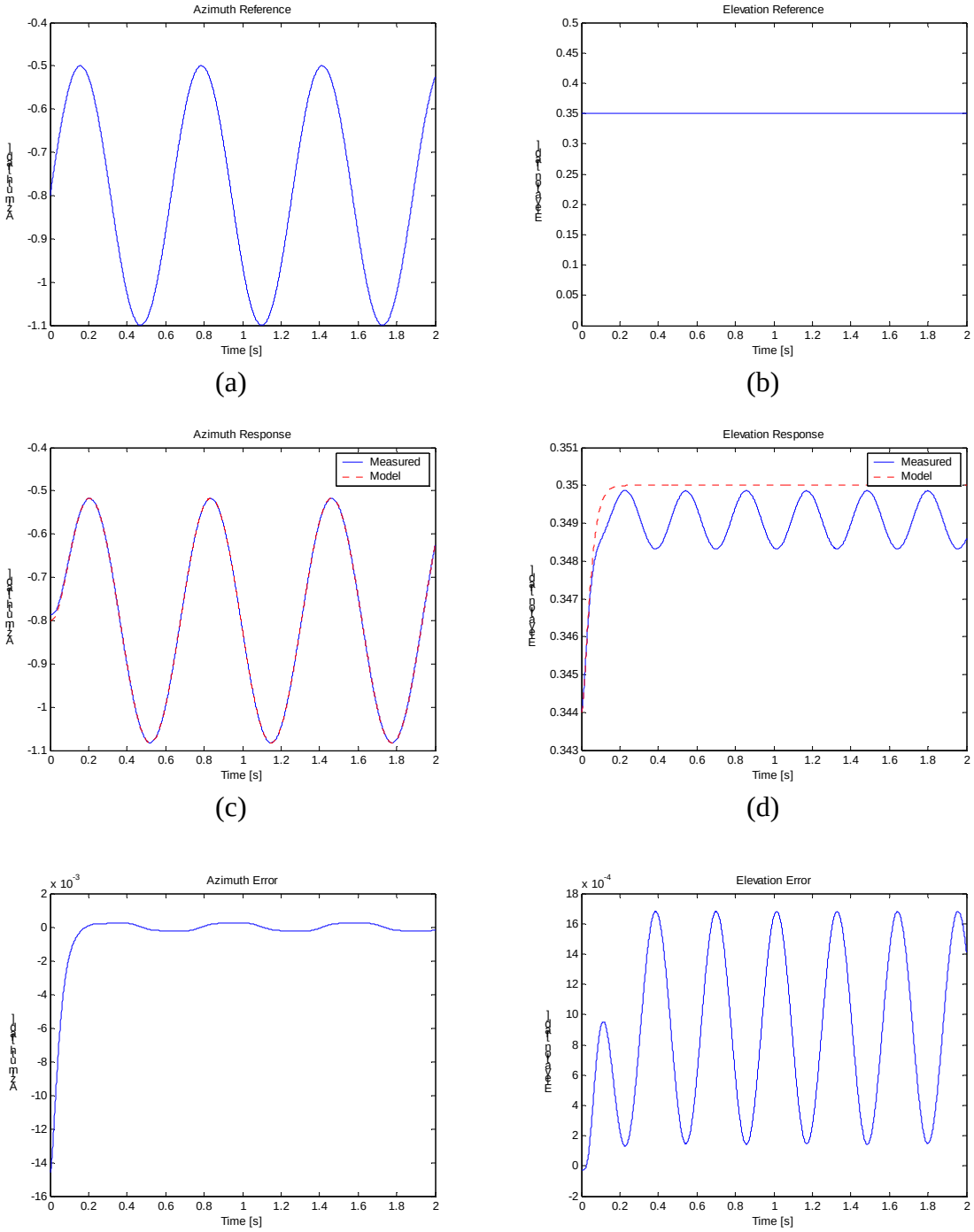

Figure 10 - State-Variable Controller Response; Reference: (a) Azimuth, (b) Declination; Response: (c) Azimuth, (d) Declination; Position Error: (e) Azimuth, (f) Declination

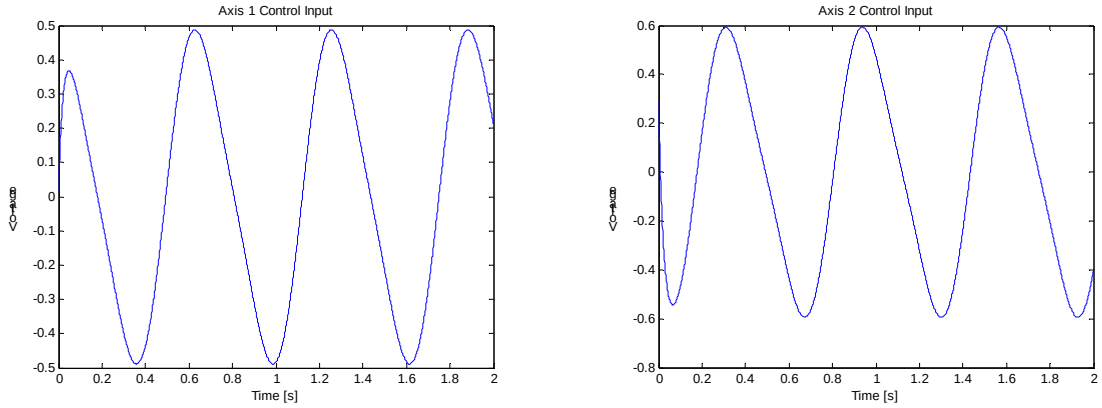

(a) (b)

Figure 11 - Control Signals Produced by the State-Variable Controller

3.3 Design, Application and Testing of an Adaptive Model Reference Controller

With the decoupling of the outputs as the main objective, a model reference adaptive controller was designed with a structure as shown in Figure 12. The reference model is driven by the azimuth and declination reference and its output adheres to the same coordinate system. Consequently, the model is decoupled. The azimuth and declination pairs are converted into motor encoder position and along with the measured encoder information serve as input to the Adaptation Mechanism (AM), which then generates the additional adaptive control inputs for both channels. The development of the Adaptation Mechanism is consistent with the approach described in [10]. The final results of the design are presented below. Figure shows a Simulink implementation of the AM given in [10].

The parameters of these equations are

$$D = \begin{bmatrix} 0.626 & 50 & 0 & 0 \\ 0 & 0 & 0.626 & 50 \end{bmatrix} \tag{11}$$

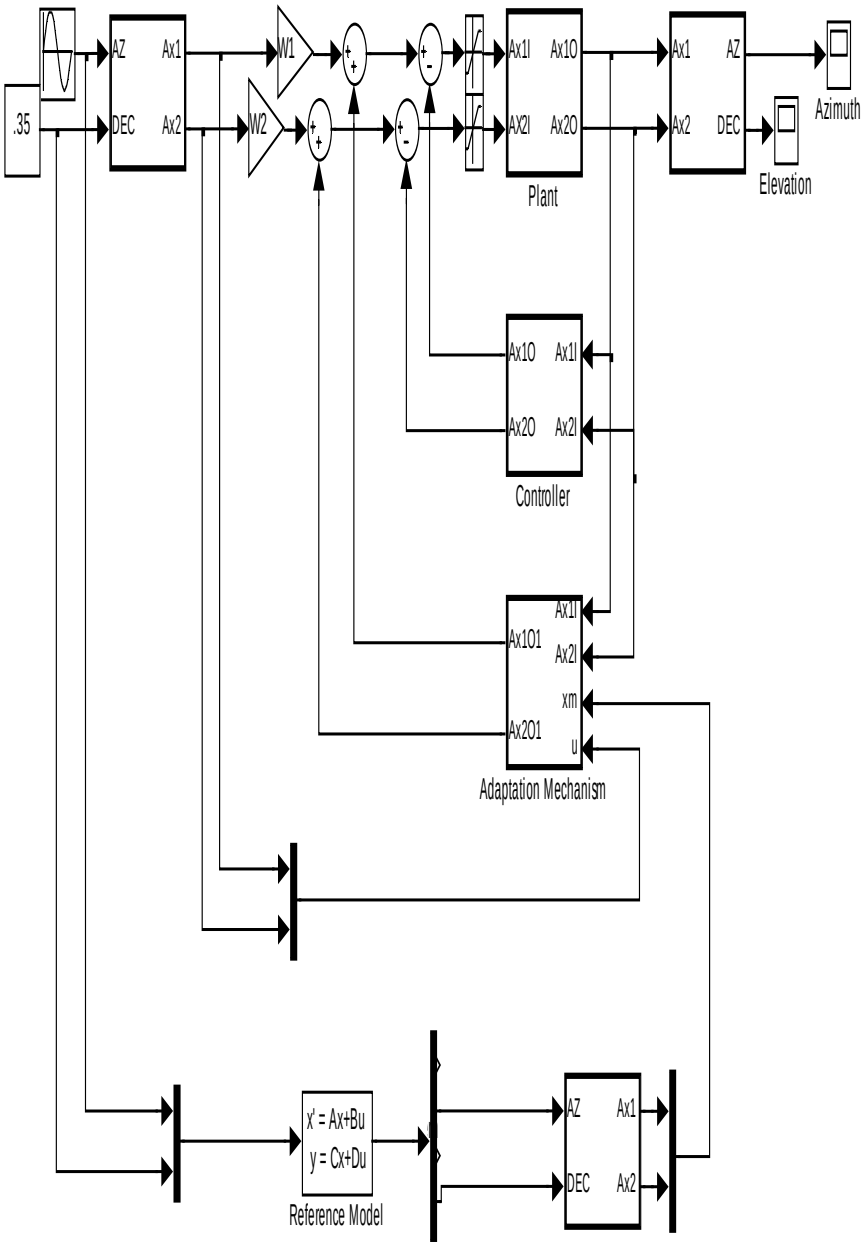

Figure 12 - System Diagram of an Adaptive Model Reference Controller

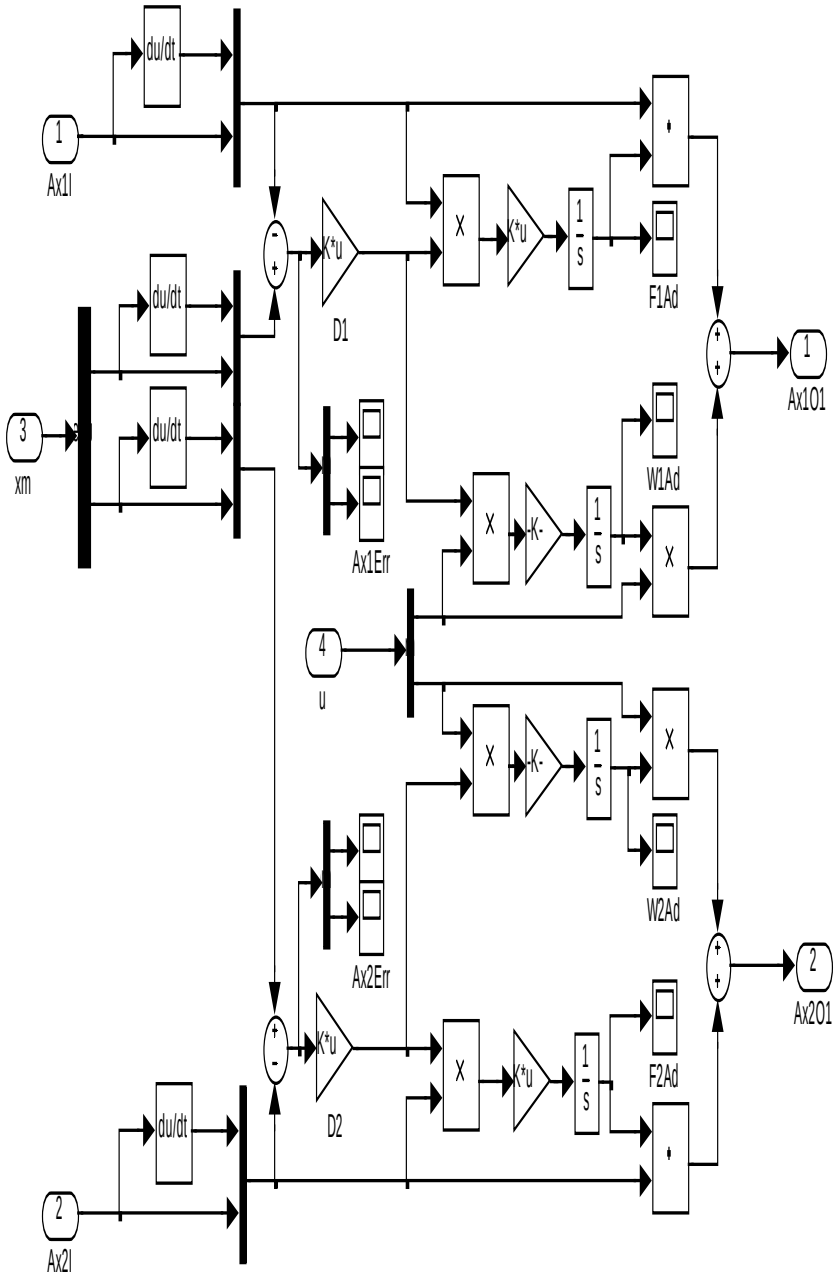

Figure 13 - Adaptation Mechanism

$$M_1 = M_3 = \begin{bmatrix} 1 & 0 \\ 0 & 1 \end{bmatrix}$$

$$N_1 = \begin{bmatrix} 10^{-12} & 0 & 0 & 0 \\ 0 & 10^{-20} & 0 & 0 \\ 0 & 0 & 5 \cdot 10^{-15} & 0 \\ 0 & 0 & 0 & 5 \cdot 10^{-13} \end{bmatrix} \tag{12}$$

$$N_3 = \begin{bmatrix} 5 \cdot 10^{-11} & 0 \\ 0 & 5 \cdot 10^{-11} \end{bmatrix}$$

$$M_2 = M_4 = N_2 = N_4 = 0$$

The performance of the adaptive controller is captured in Figure 14. After the initial oscillations die out, the tracking error is kept very close to zero. The control signals produced by the state-variable controller and by the AM are show in Figure 15. The adaptation of parameters ΔF and ΔW is show in Figure 16. In the simulation diagrams and plots, matrices F_1, F_2, W_1 and W_2 constitute matrices F and W as follows

$$F = \begin{bmatrix} F_1 & 0 \\ 0 & F_2 \end{bmatrix}$$

$$W = \begin{bmatrix} W_1 & 0 \\ 0 & W_2 \end{bmatrix}. \tag{13}$$

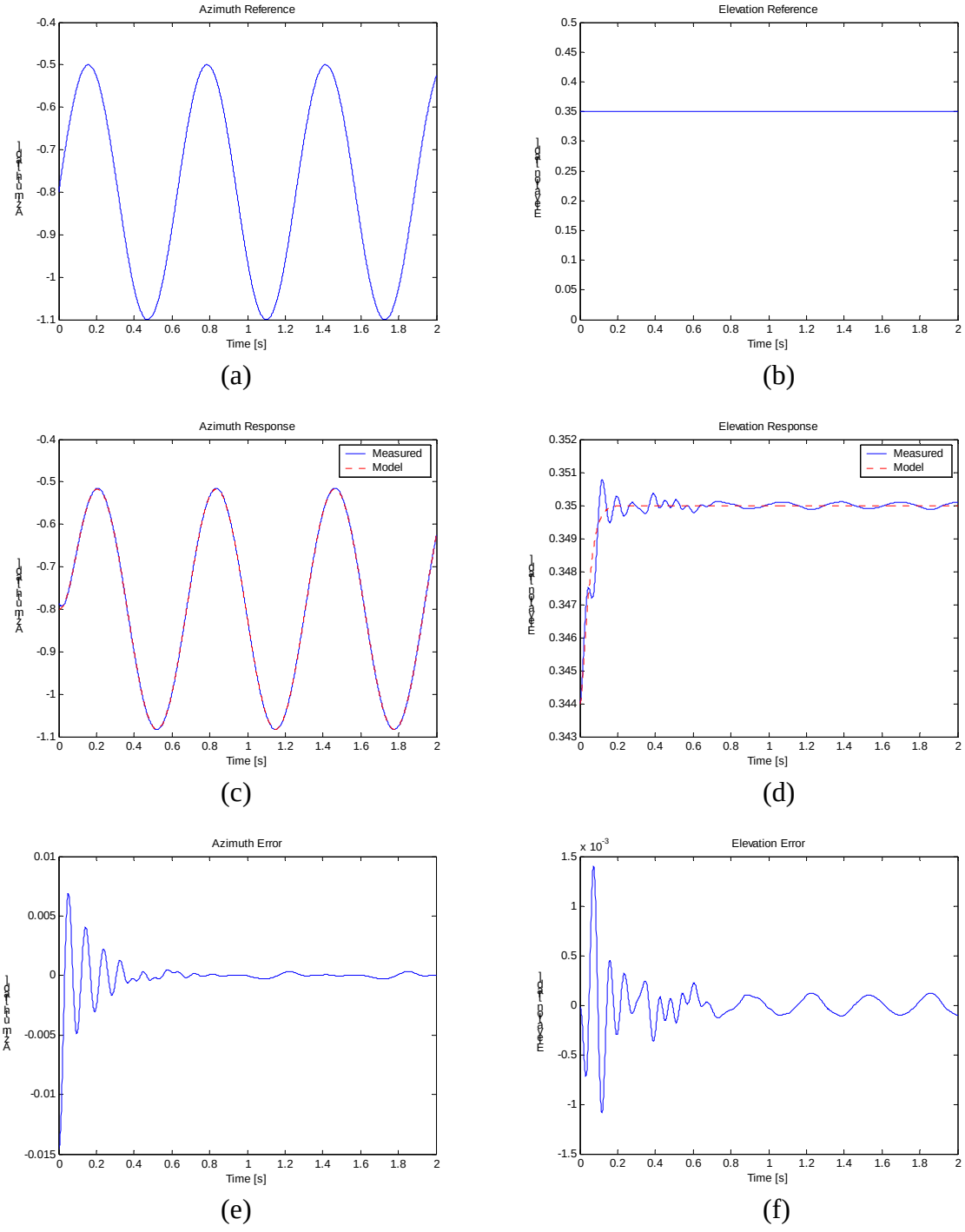

Figure 14 - Adaptive Model Reference Controller Response; Reference: (a) Azimuth, (b) Declination; Response: (c) Azimuth, (d) Declination; Position Error: (e) Azimuth, (f) Declination

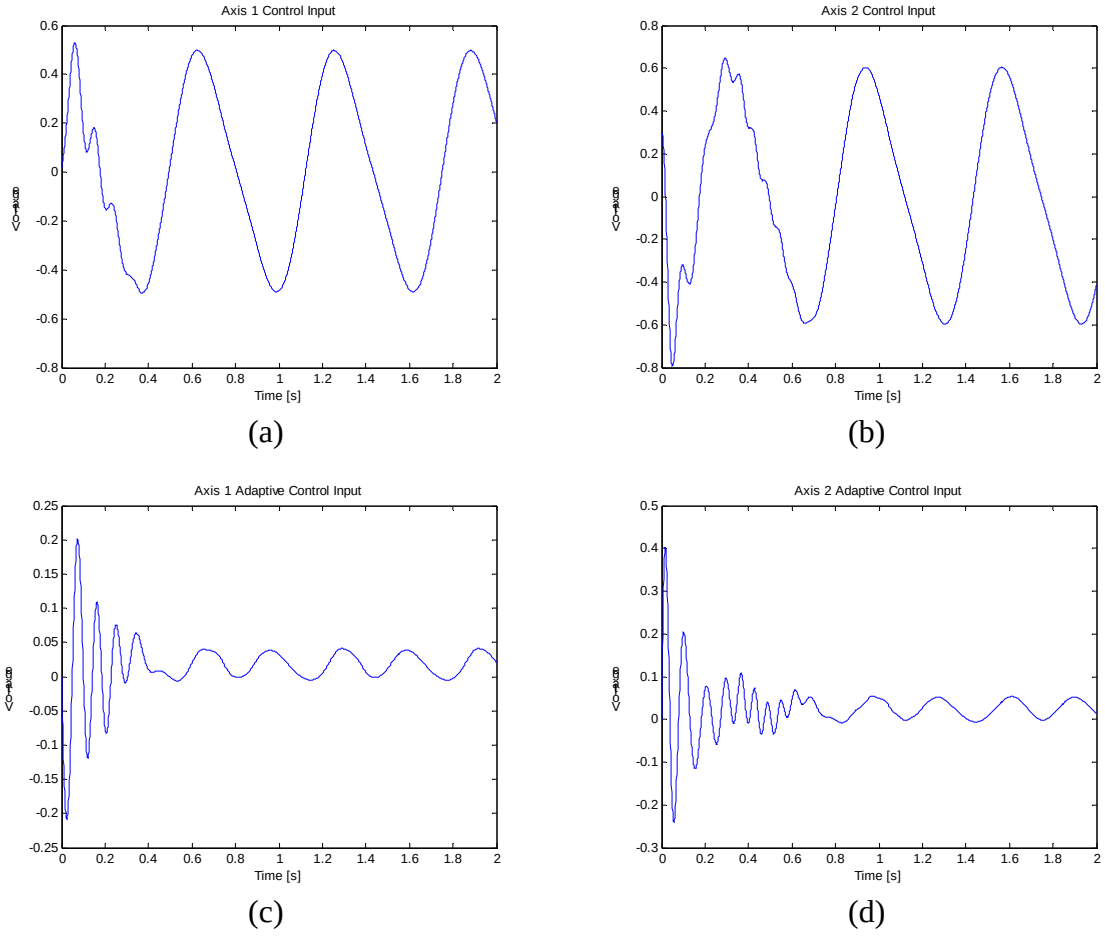

Figure 15 - Control Signals Produced by the State-Variable Controller (a) and (b); and by the Adaptation Mechanism (c) and (d)

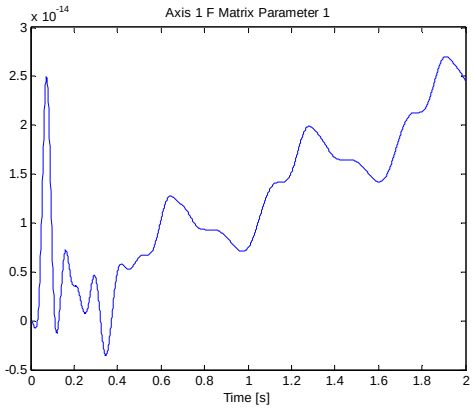

(a)

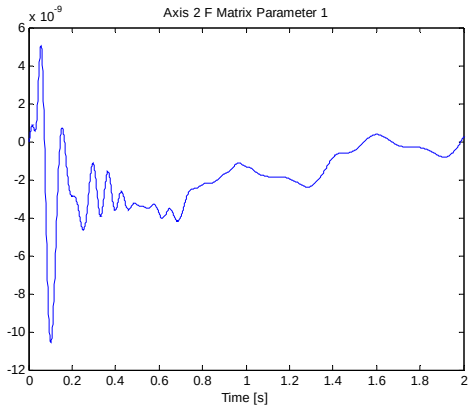

(b)

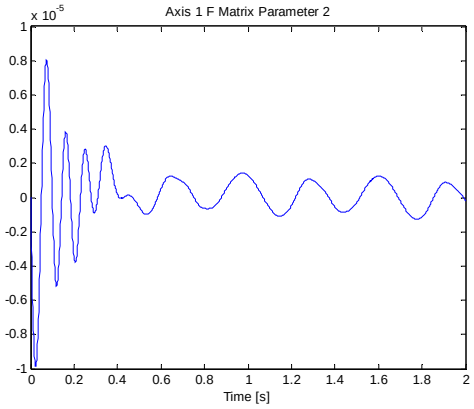

(c)

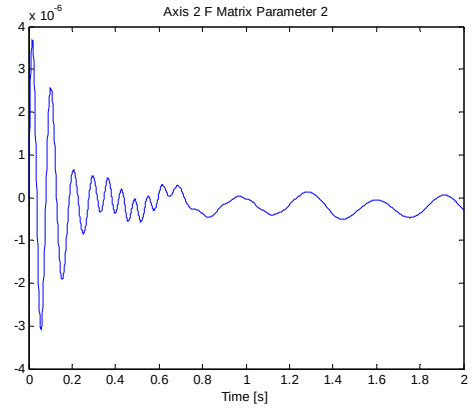

(d)

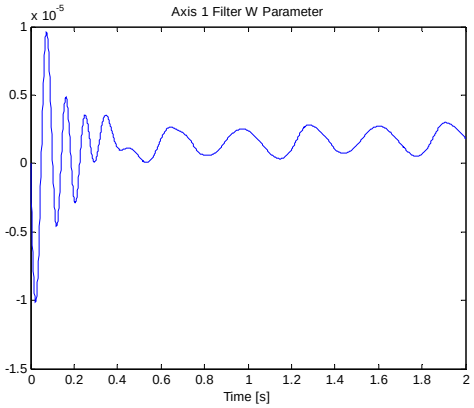

(e)

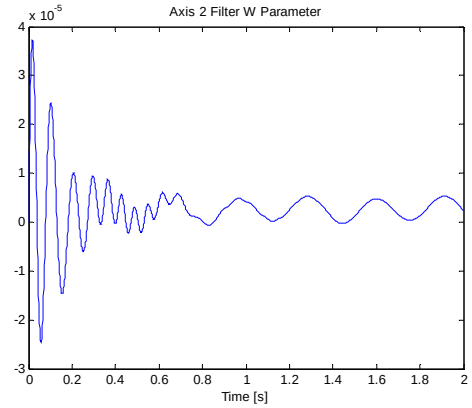

(f)

Figure 16 - Adaptation of Parameters of Matrix F (a), (b), (c) and (d), and of Matrix W (e) and (f)

3.4 Comparative Analysis of the Control Laws: Complexity vs. Functionality

As it was mentioned earlier, the inaccessibility of key signals in the original controller setup made detailed analysis and performance assessment unrealizable. Therefore, this section will focus on the two controllers developed in Sections II.2 and II.3. A direct comparison between of Figure 10 (d) and Figure (d) indicates superior decoupling capabilities of the adaptive controller. While the decoupling of the outputs through the use of a state-variable controller was fairly successful, it was mostly due to the slow variations of the reference and inherent small lag between the reference and the output. However, the introduction of an additional adaptive signal improved the response considerably, which makes a good argument for the application of adaptive control in accuracy-critical scenarios, such as high precision beam steering. Again, the cost of implementation of an adaptive controller is justifiable as in the case of friction compensation in the Schaeffer gimbals setup, due to the improved performance and relatively uncomplicated realization of the results of the adaptive control design.

4. Conclusions and Further Research

A comprehensive laboratory testing of one of few existing Omniwrist devices has resulted in the establishment of a complete transfer matrix-type model relating pitch/yaw coordinates of the sensor mount to the voltage signals applied to the motors. Although dynamic characteristics of the device are position-dependent, it has the potential for exceeding bandwidth and positioning accuracy of a traditional gimbals system at least by the factor of ten. The device is suitable for the application of the most advanced control strategies that will result in the further enhancement of its dynamic performance thus extending the scope of its application to various problems of satellite communications, LADAR, laser weapon systems, etc.

The proposed study is aimed at the investigation of the best performance characteristics (bandwidth, tracking error, cross-coupling effects, power consumption, etc.) attainable under various control laws. Model reference adaptive controller, optimal controller utilizing dynamic programming, gain scheduling, and fuzzy logic control will

be synthesized using the developed mathematical model. Implemented in software and laboratory hardware, these control strategies were tested in such typical laser positioning applications as agile repositioning of the laser beam, tracking a moving target, scanning, and offsetting vibration of the optical platform. It will demonstrate that Omniwrist III with the appropriate controls could be considered as a new generation of gimbals system.

While exceeding the bandwidth requirements for the coarse beam steering task, Omniwrist's dynamic response is much slower than the one of the acousto-optic device (Bragg cell) that is virtually inertia-less. At the same time, the steering range of a Bragg cell, ± .5°, is too small for many applications. The authors have been successful in the enhancement of the design and development of control laws improving its dynamic characteristics of a Bragg cell. We propose the research aimed at the development of a hybrid laser beam steering system comprising Bragg cells installed on the Omniwrist platform. An optimal control strategy facilitating such applications as scanning, search, rapid repositioning, tracking, feedback and feedforward compensation of environmental vibration of the optical platform (satellite-based and airborne) will be developed, implemented and tested. This includes the solution of such underlying problems as the development of the mechanical and optical systems, mathematical description of the hybrid system, optimal task distribution between the "coarse" and the "fine" positioning tasks, coordination of the operation of the "coarse" and "fine" system controllers. The efficiency of the developed system in various applications will be investigated and compared against known designs.

The **expected cost** of the proposed efforts is $60,000 over a 1.5 year period.

5. References

[1] M. E. Rosheim, G. F. Sauter, *New High-Angulation Omni-Directional Sensor Mount*," http://www.anthrobot.com/press/article_new_omni_sensor_mount.html, November, 2002

[2] "ZT 8907 Single Board Computer with IntelDX4 Microprocessor. Hardware User Manual," http://www.pt.com/Manuals_Legacy/ZT_8907_Manual.pdf, November 2002

[3] "Model 4350A 1-4 Axes STD-Bus Servo Motion Controller," datasheet, http://www.acs-tech80.com/products/legacy/4350a.pdf, November 2002

[4] "SE30A40AC Series Brushless Servo Amplifiers," datasheet http://www.a-m-c.com/download/se30a-ac.pdf, November 2002

[5] "GSX and GS Series Linear Actuator Installation and Service Manual," http://www.exlar.com/products/linear/gs/gs_pdf/gsx_gs_manual.pdf, November 2002

[6] "Sensors for High Precision Measurements," http://www.philtec.com/specsrcmetric.htm, November 2002

[7] "LS7084 Quadrature Clock Converter Datasheet," http://www.lsicsi.com/pdfs/LS7083_84.pdf, 2002

[8] M. D. Vose, *The Simple Genetic Algorithm: Foundations and Theory*, MIT Press, 1999

[9] G. Ellis, *Control System Design Guide*, 2nd ed., Academic Press, 2000

[10] Y. D. Landau, *Adaptive Control. The Model Reference Approach*, Marcel Dekker, 1979

H. Olsson, K.J. Åström, C. de Wit, M. Gäfvert, P. Lischinsky, "Friction Models and Friction Compensation," *European Journal on Control*. 1997 (http://www.control.lth.se/~kja/friction.pdf)

6 Background Literature:

[1] W. J. Palm III, *Modeling, Analysis and Control of Dynamic Systems*, John Wiley & Sons, 1983

[2] Z. Gajić, M. T. J. Qureshi, *Lyapunov Matrix Equation in System Stability and Control*, Academic Press, 1995

[3] "The Roto-Lok Drive Technology," http://sagebrushtech.com/tech/technology.html, October 2002

[4] "Application of Fiber Optics ," http://www.technology.niagarac.on.ca/courses/elnc645/notes/unit8b%20fiberapps.pdf, December 2002

[5] S. Arnon, M.-J. Montpetit, H. Hemmati, "Laser Communication Challenges and Possible Solutions," ICC 2000 Tutorial, New Orleans, June 18th 2000

[6] V. Nikulin, "Advanced Control Technologies for Laser Communications," *PhD Dissertation*, SUNY at Binghamton, NY. 2002

[7] A.Biswas, M. Wright, B. Sanii, N. A. Page, "45 km Horizontal Path Optical Link Demonstrations," http://lasers.jpl.nasa.gov/, September 2002

[8] K. E. Wilson, J. R. Lesh, "An Overview of the Galileo Optical Experiment (GOPEX)," http://lasers.jpl.nasa.gov/, September 2002

[9] H. Hemmati, K. Wilson, M. K. Sue, L.J. Harcke, M. Wilhelm, C.-C. Chen, J. Lesh, Y. Feria, "Comparative Study of Optical and Radio-Frequency Communication Systems for a Deep-Space Mission," http://lasers.jpl.nasa.gov/, September 2002

[10] T. Busch, "Beam Steering Techniques for Free Space Laser Communication," *PhD Dissertation*, SUNY at Binghamton, NY, 1997